LEVEL II

12

NRL Memorandum Report 3683
Revised

Magnetosheath Effects on Cylindrical Langmuir Probes

EDWARD P. SZUSZCZEWICZ AND PETER Z. TAKACS

Upper Air Physics Branch
Space Science Division

October 23, 1979

E. O. Hulburt Center for Space Research

NAVAL RESEARCH LABORATORY
Washington, D.C.

SECURITY CLASSIFICATION OF THIS PAGE (When Data Entered)

REPORT DOCUMENTATION PAGE

READ INSTRUCTIONS BEFORE COMPLETING FORM

1. REPORT NUMBER: NRL Memorandum Report 3683 (Revised)	2. GOVT ACCESSION NO. NRL-MR-3683
3. RECIPIENT'S CATALOG NUMBER	
4. TITLE (and Subtitle): MAGNETOSHEATH EFFECTS ON CYLINDRICAL LANGMUIR PROBES	5. TYPE OF REPORT & PERIOD COVERED: Interim report on a continuing NRL problem.
	6. PERFORMING ORG. REPORT NUMBER
7. AUTHOR(s): Edward P. Szuszczewicz and Peter Z. Takacs*	8. CONTRACT OR GRANT NUMBER(s): NASA-W14252 Sponsor Code 82728
9. PERFORMING ORGANIZATION NAME AND ADDRESS: Naval Research Laboratory Washington, D.C. 20375	10. PROGRAM ELEMENT, PROJECT, TASK AREA & WORK UNIT NUMBERS: NRL Problem A02-11
11. CONTROLLING OFFICE NAME AND ADDRESS	12. REPORT DATE: October 28, 1979
	13. NUMBER OF PAGES: 20
14. MONITORING AGENCY NAME & ADDRESS (if different from Controlling Office)	15. SECURITY CLASS. (of this report): UNCLASSIFIED
	15a. DECLASSIFICATION/DOWNGRADING SCHEDULE

16. DISTRIBUTION STATEMENT (of this Report)

Approved for public release; distribution unlimited.

17. DISTRIBUTION STATEMENT (of the abstract entered in Block 20, if different from Report)

18. SUPPLEMENTARY NOTES

*Present address: Voyager Programs, Tucson, Arizona 85713.

NRL Memorandum Report 3683 (Revised) will appear in Physics of Fluids, Vol. 22, December 1979.

19. KEY WORDS (Continue on reverse side if necessary and identify by block number)

Plasma probes
Ionospheric plasmas
Electron current collection
Magnetosheath

20. ABSTRACT (Continue on reverse side if necessary and identify by block number)

The response of cylindrical Langmuir probes in magnetoplasmas is studied from a perspective which focuses on the relative magnitudes of Larmor radius and sheath size. The approach results in a classification for magnetic field effects which involves not only the magnetic field strength but also the plasma parameters of density, temperature, and the applied probe potential. We specifically show that a 0.25 G field can have similar effects on the current collection properties of the probe in an ionospheric plasma ($N_e \approx 10^6$ cm^{-3}) as a 30 kG field would have in a hot, dense laboratory plasma ($N_e \approx 10^{15}$ cm^{-8}). The classifications are found to agree with new experimental results collected in

(Continues) → next page

N sub e approx. = 1,000,000/cu.cm.

N sub e approx. = 10 to the 15th power / cu.cm.

251 950

20. ABSTRACT (Continued)

an ionospheric plasma. The data also show: (a) the effects of probe orientation on electron current collection from magnetoplasmas; (b) that these effects can be important even when the electron Larmor radius is larger than the radius of the probe; and (c) that substantial magnetic field effects occur when the probe's sheath is comparable to or greater than the Larmor radius.

CONTENTS

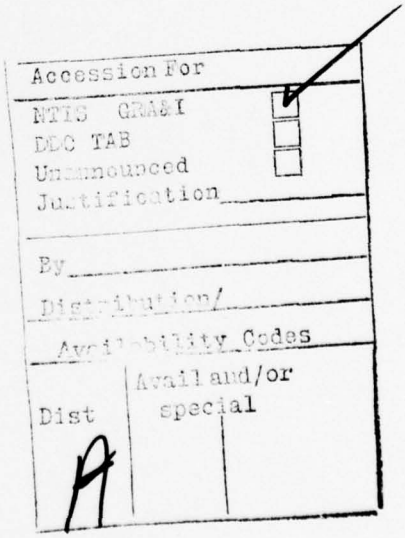

MAGNETOSHEATH EFFECTS ON CYLINDRICAL LANGMUIR PROBES

I. INTRODUCTION

The Langmuir probe is one of the most widely used diagnostic tools in laboratory and space plasmas, largely because of its apparent simplicity and the extensive documentation of its operational characteristics. However, its apparent operational simplicity belies potential pitfalls which can seriously degrade its diagnostic capability and associated determinations of plasma density and temperature[1-7]. Some appreciation for potential problems can be achieved by recognizing that the current-voltage (I-V) characteristic of the probe is a function of the size, geometry, and surface condition of the probe, as well as the probe voltage, the ambient magnetic field, and the plasma properties of the charged-particle number densities, particle distribution functions, and collision frequencies.

The determination of density and temperature from the probe's I-V characteristic hinges on the experimenter's ability to accurately account for the varying parametric influences and to overcome such experimental difficulties as plasma depletion, contamination, and area effects. If one assumes that all experimental sources of error have been eliminated, the accuracy of the technique is limited by the theoretical description of the probe's response under the prevailing plasma conditions. Under these circumstances, the most difficulty is encountered when the operation of the probe is in any one of the various transition regions, where we use the term "transition region" to describe any domain between the mathematically convenient limits of collision-free and collision-dominated, thin-sheath and thick-sheath, and strong-field and weak-field. These regions are particularly difficult to describe because one must account for detailed charged-particle trajectories that have no convenient mathematical form as they traverse the region between the undisturbed plasma volume and the probe surface. In this work we look at the transition-region of

Manuscript submitted July 27, 1979.

magnetic field effects and the associated response of cylindrical Langmuir probe electron-saturation currents.

Probe response in magnetoplasmas can be grouped into three broad categories defined by the relative magnitudes of the probe radius R_p, the sheath thickness $(R_s - R_p)$, and the Larmor radii for electrons (R_L^e) and ions (R_L^i). We define these categories as:

$$R_p, (R_s - R_p) \ll R_L^{e,i} \quad \text{(weak-field)} \tag{1a}$$

$$R_p, (R_s - R_p) \gg R_L^{e,i} \quad \text{(strong-field)}, \tag{1b}$$

and

$$R_p, (R_s - R_p) \approx R_L^{e,i} \quad \text{(transition-field)}. \tag{1c}$$

Each of these categories has its own morphological subdivision established by the independent ratios $R_L^{e,i}/R_p$ and $R_L^{e,i}/(R_s - R_p)$. The first ratio, $R_L^{e,i}/R_p$, involves geometrical effects which result in magnetic field shadowing[8] and the associated perturbation of a fully-Maxwellian plasma distribution at the sheath edge. A number of authors[2, 9-12] have used this ratio to describe magnetic field effects on cylindrical probes and have shown reduced saturation currents when the ratio was small. Miller[11] and Laframboise and Rubinstein[12], however, infer that magnetic field effects may occur even when $R_L^{e,i} \gg R_p$ if $R_L^{e,i} \lesssim (R_s - R_p)$. It is the latter inequality which is of primary concern in the present investigation.

Arguments advanced in subsequent sections point out that the interrelationships between R_p, $R_L^{e,i}$, and $(R_s - R_p)$ are all important in establishing the probe's response in the presence of magnetic fields. Our results demonstrate the important role of sheath size in the case of moderate-to-weak magnetic fields and point to possible errors that can arise in attempts to monitor relative electron (ion) densities by changes in electron- (ion-) saturation currents. We specifically show that, in general, one cannot assume $I_e \propto N_e$ when probe operation is in the transition region of magnetic field effects.

II. SHEATH CONSIDERATIONS

A. *Sheath size.* In describing magnetic field effects on probes it is necessary to establish an understanding of the plasma sheath which envelopes the probe and controls the charged-particle fluxes as they move from the undisturbed plasma volume to the collecting surface of the probe. Typically, the electron Debye length λ_D is used as a convenient approximation for the sheath size, but, this approach has limited accuracy and does not include sheath dependence on probe potentials. We will therefore extract from the numerical calculations of Laframboise[13] an analytical relationship for the plasma sheath size which will be applied to our model of magnetic-field effects on cylindrical probes.

The Laframboise calculations are based on the Boltzmann-Vlasov equation for Maxwellian electrons and ions, coupled with Poisson's equation and the boundary condition

$$\left(\frac{d\varphi}{dR}\right)_{R_b} = -\left(\frac{\varphi}{R}\right)_{R_b} \tag{2a}$$

for the solution in the case of cylindrical probes. (Additional discussions of Laframboise's calculations can be found in the works of de Leeuw[14], Sonin[15], and Szuszczewicz[5].) For electron-attracting probe potentials in the limit of zero-temperature ions the boundary condition is relaxed and replaced by

$$\left(\frac{d\varphi}{dR}\right)_{R_b} = \left(\varphi\right)_{R_b} = 0. \tag{2b}$$

In this case R_b is a sharp boundary defined as the sheath edge radius where the repelled ion spatial distribution is discontinuous [i.e., $(N_i)_{R < R_b} = 0$ and $(N_i)_{R > R_b} = N_e$]. In the computational scheme the sheath radius was not known in advance, but its position was adjusted until the total space charge within the sheath exactly canceled the charge on the probe. The resulting boundary value problem then required solutions for the potential and charge density distributions as well as the position of the sheath edge $R_b (\equiv R_s)$. The

analytic expression which we have fit to the resulting Laframboise calculations (Fig. 38, Ref. 13) for the dimensionless sheath thickness S is given by

$$S = \frac{R_s - R_p}{\lambda_D} = \left[2.50 - 1.54 \exp(-0.32 R_p/\lambda_D) \right] \left(\frac{e\varphi_p}{kT_e} \right)^{1/2} \tag{3}$$

This function is plotted in Fig. 1. Comparison of Eq. (3) with the calculations of Laframboise[13] showed agreement to be within a few percent for $R_p/\lambda_D \leq 10$. The difference increases to 26% at $e\varphi_p/kT_e = 25$ in the limit of $R_p/\lambda_D \rightarrow \infty$; but this deviation is inconsequential.

Figure 1 also includes calculations for sheath radius based on the analysis of Bettinger and Walker[16] for cylindrical electron-attracting probes. Their analysis does not provide the potential distribution within the sheath. Instead, they consider the probe surface and sheath edge as concentric electrodes of a cylindrical capacitor and assume the charge density within the sheath to be inversely proportional to the local velocity of the incoming particles. The probe surface charge is then equated to the total charge within the sheath with the resulting expression demonstrating the dependence of sheath size on probe radius, Debye length, and applied probe potential. Although their results do not bear the rigor of the Laframboise calculations, they do provide an alternate description of the sheath edge radius that includes dependence on probe potential and radius rather than a simple identification with Debye length. (It should be noted that Eq. (14) in the work of Bettinger and Walker[16] is in error by a constant. $(s^2 + 2\rho s)\ln(1 + s/\rho) = \pi \ \psi_s(1 + \frac{2}{3}\psi_s)^{1/2}$ should be $(s^2 + 2\rho s)\ln(1 + s/\rho) = 2\psi_s(1 + \frac{2}{3}\psi_s)^{1/2}$. The corrected form has been utilized in the current work.)

Of the two approaches, the Laframboise results represent a more realistic physical model with a solution scheme that includes the dependence of sheath potential distribution and the associated charge profile on the geometry of the probe. It is the Laframboise approach with the analytical description provided by Eq. (3) which is utilized in this work.

B. *Magnetic field effects.* No attempt will be made to establish an anisotropic description of sheath geometry, an effort which goes beyond the scope of this work. In this section we

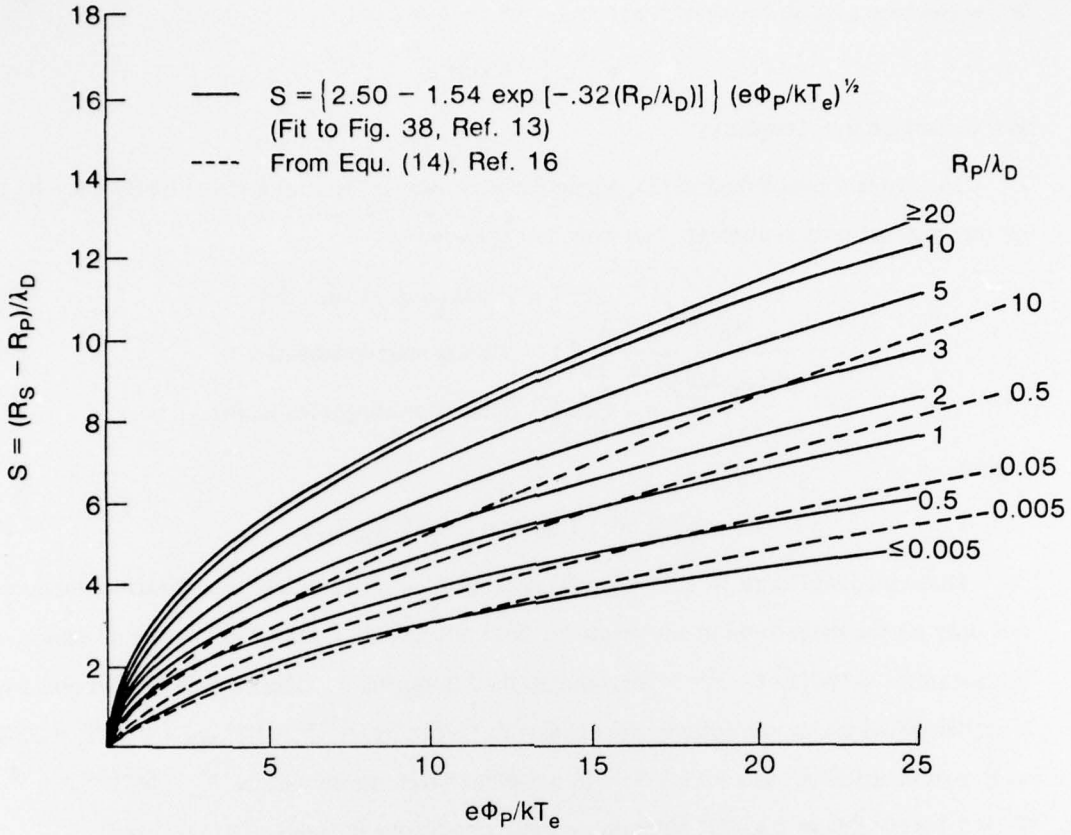

Fig. 1 — Dimensionless sheath size vs normalized probe potential

establish criteria which determine the combined effects of magnetic field strengths and sheath size on electron saturation currents.

With the use of Eq. (3) guidelines can be determined for the inequalities (1a)-(1c) by examining the ratio $R_L^e/(R_s - R_p)$. This ratio can be written as

$$\frac{R_L^e}{R_s - R_p} = \frac{\omega_p^e/\omega_c^e}{2.50 - 1.54 \exp[-0.32R_p/\lambda_D]) (e\varphi_p/kT_e)^{1/2}} \tag{4}$$

where

$$\omega_p^e = (4\pi Ne^2/m_e)^{1/2} \tag{5}$$

is the electron plasma frequency, and

$$\omega_c^e = eB/m_e c \tag{6}$$

is the electron gyrofrequency.

The criteria established in (1), particularly as they apply to the effect of $R_L^e/(R_s - R_p)$ on electron saturation currents, can now be expressed as

$$\frac{\omega_p^e/\omega_c^e}{F(e\varphi_p/kT_e)^{1/2}} \begin{cases} \gg 1 & \text{(weak-magnetosheath)} \quad (7a) \\ \ll 1 & \text{(strong-magnetosheath)} \quad (7b) \\ \approx 1 & \text{(transition-magnetosheath)} \quad (7c) \end{cases}$$

where

$$F = 2.50 - 1.54 \exp(-0.32\, R_p/\lambda_D). \tag{8}$$

These inequalities show that a weak-, transition-, or strong-field classification depends not only on the magnitude of the magnetic field but also on plasma parameters of density and temperature, as well as the probe size and applied potential φ_p. Thus a 0.25 G field could have a similar effect on an ionospheric plasma sheath (typically, $N_e^{max} = 10^6$ cm^{-3} and $T_e = 2000°$K at F- region altitudes) as a 30 kG field in a confined hot, dense plasma [$N_e = 5(10^{15})$cm^{-3}, $T_e = 1.16(10^7)°$K (= 1 keV)]. Examining these conditions in terms of (7) we find

$$\frac{\omega_p^e/\omega_c^e}{F(e\varphi_p/kT_e)^{1/2}} = 4 \tag{9}$$

in the ionospheric case, and

$$\frac{\omega_p^e/\omega_c^e}{F(e\varphi_p/kT_e)^{1/2}} = 0.95 \tag{10}$$

for the hot, dense plasma. These results assume $e\varphi_p/kT_e = 10$ as a nominal operational value for the collection of electron saturation currents by a cylindrical probe of radius $R_p = 3.8(10^{-2})$ cm. Since Eqs. (9) and (10) are of comparable magnitude, their results show that dramatically different probe-plasma systems can have similar classifications with regard to magnetosheath effects.

C. *Angular dependence.* The anisotropic nature of charged-particle motion makes it necessary to consider the field direction $\hat{B}$ relative to the probe and sheath axes $\hat{L}$. The most complete work done to date in this area is that of Laframboise and Rubinstein[12] who have conducted a theoretical analysis of a cylindrical probe in a collisionless plasma, with the probe operating under thick sheath conditions at an arbitrary angle $\theta \left[\equiv \cos^{-1}\left(\overline{L}\cdot\overline{B}/LB\right)\right]$ with respect to a uniform magnetic field. For a probe at plasma potential, their analysis is exact; but in regions of electron saturation currents their theory provides only an upper bound and an adiabatic limit. These limits are approached, respectively, at larger and smaller values of R_L^e/L_φ, where L_φ is defined by Laframboise and Rubinstein as the gradient scale length of sheath potential $\varphi/|\nabla\varphi|$. The adiabatic limit corresponds to $R_L^e/L_\varphi \to 0$ and can be represented approximately by $R_L^e/(R_s - R_p) \to 0$.

The Laframboise and Rubinstein adiabatic calculations show that $I_e(\theta_a)/I_e(\theta_b) < 1$ for $\theta_a < \theta_b$. A sample of their electron-current calculations at plasma potential ($e\varphi_p/kT_e = 0$) and in the saturation regime ($e\varphi_p/kT_e = 5$) is presented in Fig. 2. All results are normalized to fully Maxwellian current levels collected at plasma potential under zero magnetic field conditions. In the next section we present our experimental results for comparison with theory and discuss the role of $R_L^e/(R_s - R_p)$ in approaching the adiabatic limit.

III. EXPERIMENTAL RESULTS

A. *Experimental configuration.* The experimental results were collected by a pulsed-plasma-probe (P^3) flown on a scientific rocket payload (NASA 18.170) into the equatorial ionosphere above Lima, Peru. The P^3 technique utilizes a special pulse procedure for generating Langmuir-probe current-voltage characteristics. The procedure reduces possible perturbations of the measurement technique by surface contamination[6, 17] and makes possible a determination of electron density and temperature under fluctuating plasma conditions[18-20].

Current-voltage characteristics were generated by voltage pulses ($\approx$ 100 μsec) which followed a sawtooth envelope from −1.6 V to + 3.0 V. During the interpulse period ($\approx$ 1.6 msec) the probe potential was held at a fixed baseline value V_B in order to stabilize

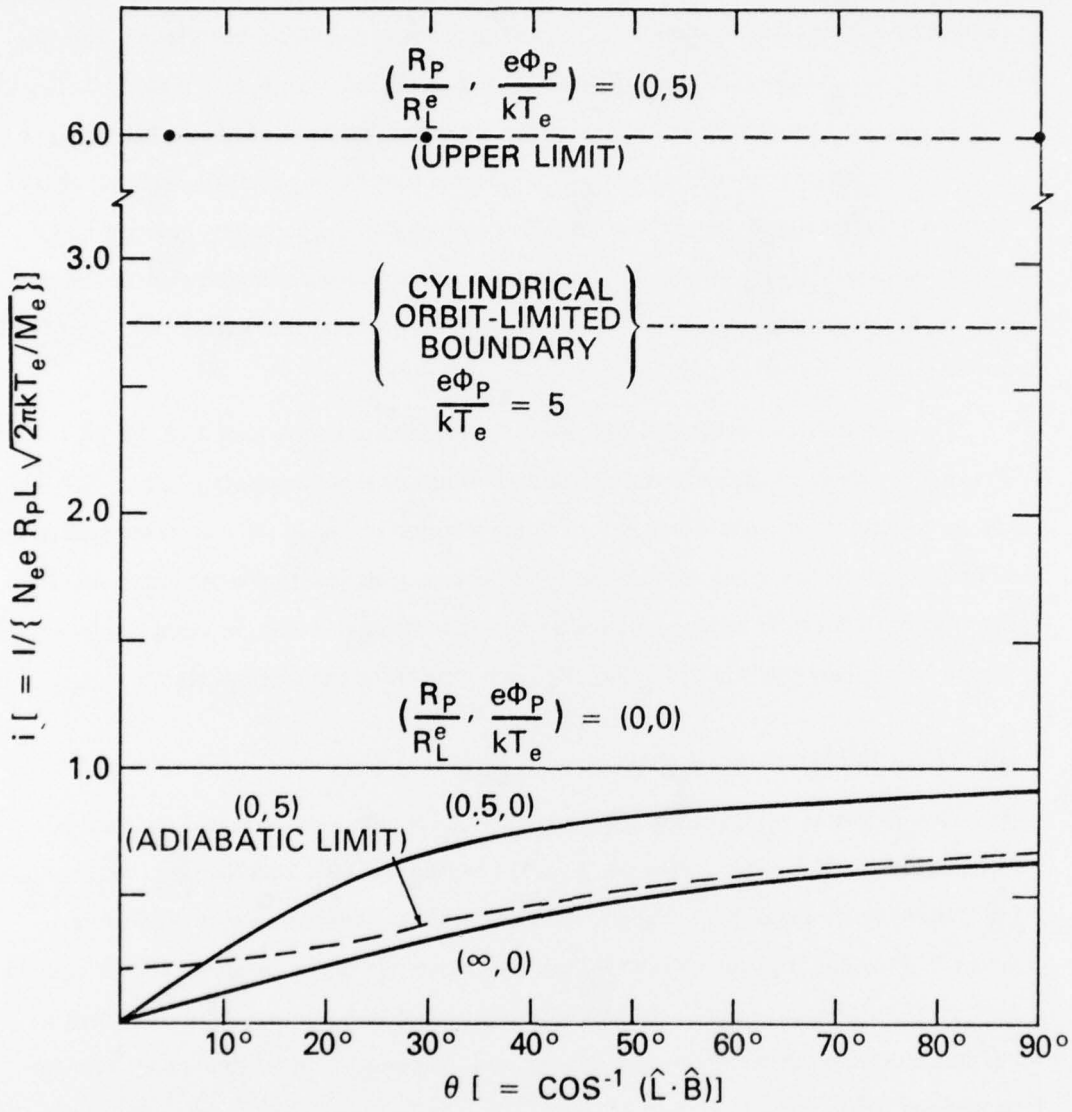

Fig. 2 — Effect of probe orientation on electron current collection in a magnetic field [12]

probe-surface conditions. Changes in probe current which might occur independent of sweep voltage were tracked by a current measurement I_B during the time of the blanked fifth pulse[6, 17]. With V_B = + 2.0V, I_B collection took place in the electron saturation portion of the I-V characteristic. (In more recent applications[21], the fifth pulse has been restored and I_B -measurements have been performed during every interpulse period at $V = V_B$.)

A redundant pair of probes was flown on the Nike-Tomahawk payload. Each probe was constructed of a 0.076 cm diam tungsten rod 20.3 cm in length. In its deployed configuration the probe was perpendicular to the spin axis of the payload and separated from its 39.4 cm boom by a coaxial guard electrode that was 1.3 cm long and 0.32 cm in diameter. The guard was simultaneously driven with the same voltage as the probes.

The payload was launched from the Chilca Range in a trajectory that was 4° north of due west. With the range located at the magnetic equator and the geomagnetic field inclined at 4° east of north, the payload trajectory was perpendicular to the magnetic field. To maintain aspect stability the payload was spun at a rate of 4 rps. The spin axis of the payload was inclined at 10° from local vertical with an estimated coning angle less than 5°. As a result, each probe was rotated from $0°(^{+5°}_{-0°})$ to $90°(\pm 0°)$ with respect to the magnetic field twice during each spin period.

B. *Results.* To measure the dependence of $I_B(= I_e^{sat})$ modulation on ionospheric plasma parameters we have plotted in Fig. 3 values of I_B at $\theta = 0°$ $(^{+5°}_{-0°})$ and $\theta = 90°$ $(\pm 0°)$. Using the $I_B(\theta = 90°)$ profile as the more accurate measure of relative density[11] and establishing the conversion $N_e(cm^{-3}) = 1.25\ (10^{11})I_B$ (A), Fig. 3 demonstrates the importance of plasma density (through its control of sheath size) in determining the effect of magnetic fields on electron current collection by cylindrical Langmuir probes. (The N_e/I_B proportionality was determined near apogee by conventional analysis[2] of the electron-saturation portion, I_e^{sat}, of the current-voltage characteristic, i.e., $d(I_e^{sat})^2/d\varphi_p \rightarrow N_e$. The simultaneous measurement of N_e and I_B, made possible with the P^3 technique, yielded the constant. Sources of error identified with possible plasma depletion[7], surface

contamination[17-18], reference electrode area[5], and convective effects[1] were inconsequential.) In the ionospheric E-region trough (125 - 170 km) where the plasma density is lowest $\left[\approx 6.0(10^3)\ \mathrm{cm}^{-3}\right]$ the percent modulation, $M \equiv \left\{[I_B(90°) - I_B(0°)]/I_B(90°)\right\} \times 100\% = 75\%$, is much greater than in the F region ($Z > 170$ km) where the modulation is only 10-15%. The difference is attributed to sheath size variation since over the altitude range in this investigation the earth's magnetic field and associated Larmor radii are approximately constant. (R_L values are constant only if temperatures are constant, a situation which is not generally true over this altitude range where we can expect up to a factor of two difference. But we can neglect the temperature effect (2×) compared to the density effect (×100).)

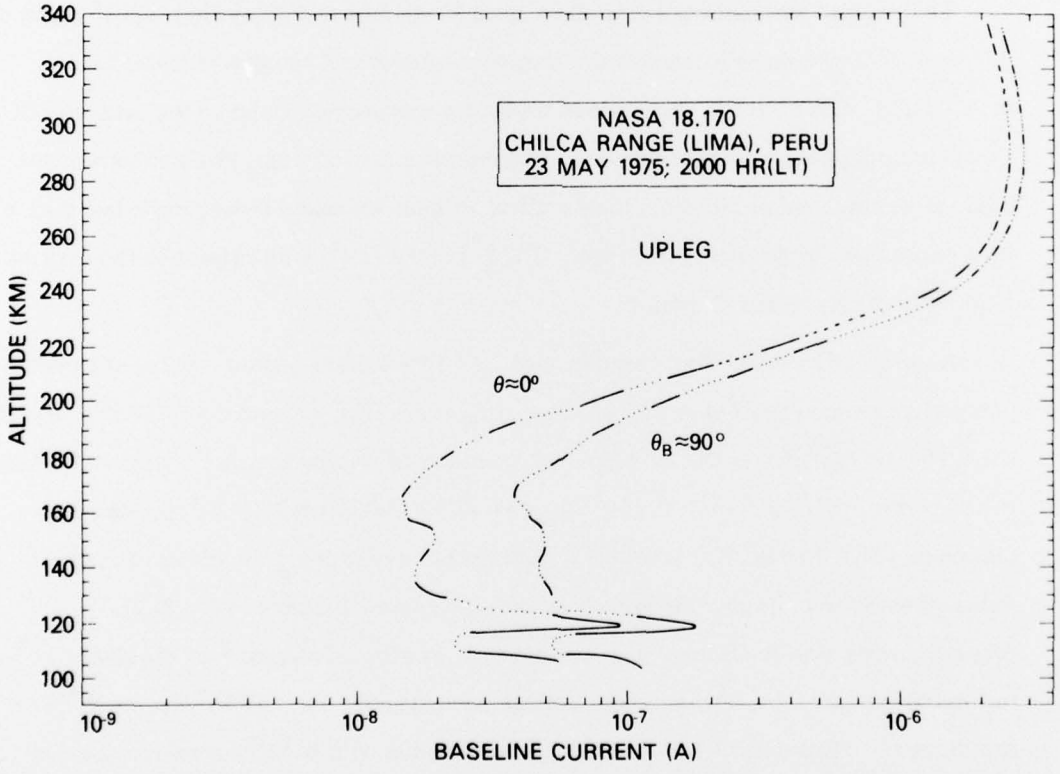

Fig. 3 — Baseline current I_B collected when the probe was at 0° ($^{+5°}_{-0°}$) and 90° with respect to the geomagnetic field

The results in Fig. 3 identify a potential problem area for plasma experimenters who utilize fixed bias cylindrical probe measurements of electron-saturation currents to determine changes in electron density. Even when the probe is held at a fixed angle with respect to the magnetic field, the spatial or temporal profile of plasma density can be distorted by changing sheath sizes that accompany varying plasma densities. Distorted data can result in misleading interpretations of active physical principles. In Fig. 3 the $I_B(\theta = 0°)$ curve could lead to erroneous conclusions concerning nighttime E-region depletion mechanisms (130-170 km) or applicability of the electron density gradient at the bottom-side of the F layer (170-240 km) to the Rayleigh-Taylor instability and the triggering of ionospheric plasma irregularities.

That reasonable levels of measurement integrity can still be maintained in weak magnetoplasmas has been indicated by Miller[11], and Laframboise and Rubinstein[12]. Their works indicate that accuracy is improved in cylindrical probe measurements when the angle between the probe and the magnetic field is large ($\theta \gtrsim 60°$). This is particularly true in the case $e\varphi_p/kT_e = 0$ and $R_p/R_L^e \leqslant 0.5$ as shown by the solid curves in Fig. 2. (The cylindrical orbit-limited boundary is included in the figure because it is a realistic upper-bound that should not be exceeded. Laframboise and Rubinstein make this point in their discussion.)

Three cases have been selected from our ionospheric data to detail the behavior of $I_B(\theta)$ as a function of plasma density. The results have been normalized to $I_B(90°)$ and plotted in Fig. 4 as curves A, B, and C. We note that the modulation increases with decreasing N_e, a parametric dependence not shown in current theories involving thick sheath conditions ($R_p/\lambda_D \ll 1$). Specifically, we find that $(\omega_p^e/\omega_c^e)/F\left(e\varphi_p/kT_e\right)^{1/2}$ $\left[= R_L^e/(R_s - R_p)\right]$ equals 2.5, 0.47, and 0.3 for A, B, and C, respectively. In terms of the inequalities in (7) these cases qualify as transition-magnetosheath. We observe that the $R_L^e/(R_s - R_p) = 2.5$ case has the smallest modulation since it approaches the condition of weak-magnetosheath. The data show that the modulation would not be zero as a result of $R_p/R_L^e \to 0$ alone. The modulation can be zero only if R_p/R_L^e and $(R_s - R_p)/R_L^e$ both go to zero, a combined condition represented by $R_L^e/(R_s - R_p) \gg 1$ [Eq. (7a)] in the thick sheath limit. The data demonstrate the important coupling of B, N_e, T_e, and φ_p in

determining the degree to which magnetic fields perturb electron current collection. One cannot give sole consideration to R_p/λ_D or R_p/R_L^e, but rather their important interrelationships as described in Eq. (7).

C. *Comparison with theory.* Figure 4 includes the upper bound (U) and adiabatic limit (L) predictions of Laframboise and Rubinstein with parametric dependence on R_p/R_L^e. The adiabatic limit results are based on two models. For non-zero values of R_p/R_L^e the calculated current results from a detailed study of the intersections of helical orbits with an infinitely long probe. Current is collected only from positive-total-energy orbits that originate at infinity rather than elsewhere on the probe. The particles are assumed to have a "one-dimensional" velocity distribution in which kinetic energy gain from the applied field goes entirely into increased speed along $\vec{B}$. In this model all possible collection orbits are empty and the associated probe current is zero when the probe axis is parallel to $\vec{B}$. The calculations of Laframboise and Rubinstein for $R_p/R_L^e = 0.1$, 1.0, and 10 are shown in Fig. 4 with extrapolations to $\theta = 0°$.

At $R_p/R_L^e = 0$ a different approach is employed by Laframboise and Rubinstein. As already noted, the current is calculated in the limit in which the velocity distribution of incoming particles at the probe is "one-dimensional"; but, instead of detailed orbital considerations, their scheme is reduced to calculating the current collection of particles with orbits of negligible curvature that flow along magnetic flux tubes intersecting the probe. The currents are allowed to have components from particle velocities both perpendicular and parallel to $\vec{B}$. This is an important difference since it allows current collection even with the probe aligned with $\vec{B}$. Compared with the calculations at $R_p/R_L^e \neq 0$, the approach at R_p/R_L^e, $\theta = 0$ effectively eliminates the emptying of collection orbits by previous intersections with an infinitely long probe. The result, as shown in Fig. 4, is a finite nonzero value for current when the probe is parallel to $\vec{B}$. In a real situation with a probe of finite length, collection orbits at $\theta = 0°$ would be partially filled by particles entering the sheath at the probe ends. One would therefore expect current collection at small values of θ and R_p/R_L^e to be bracketed between the predictions of the two computational schemes.

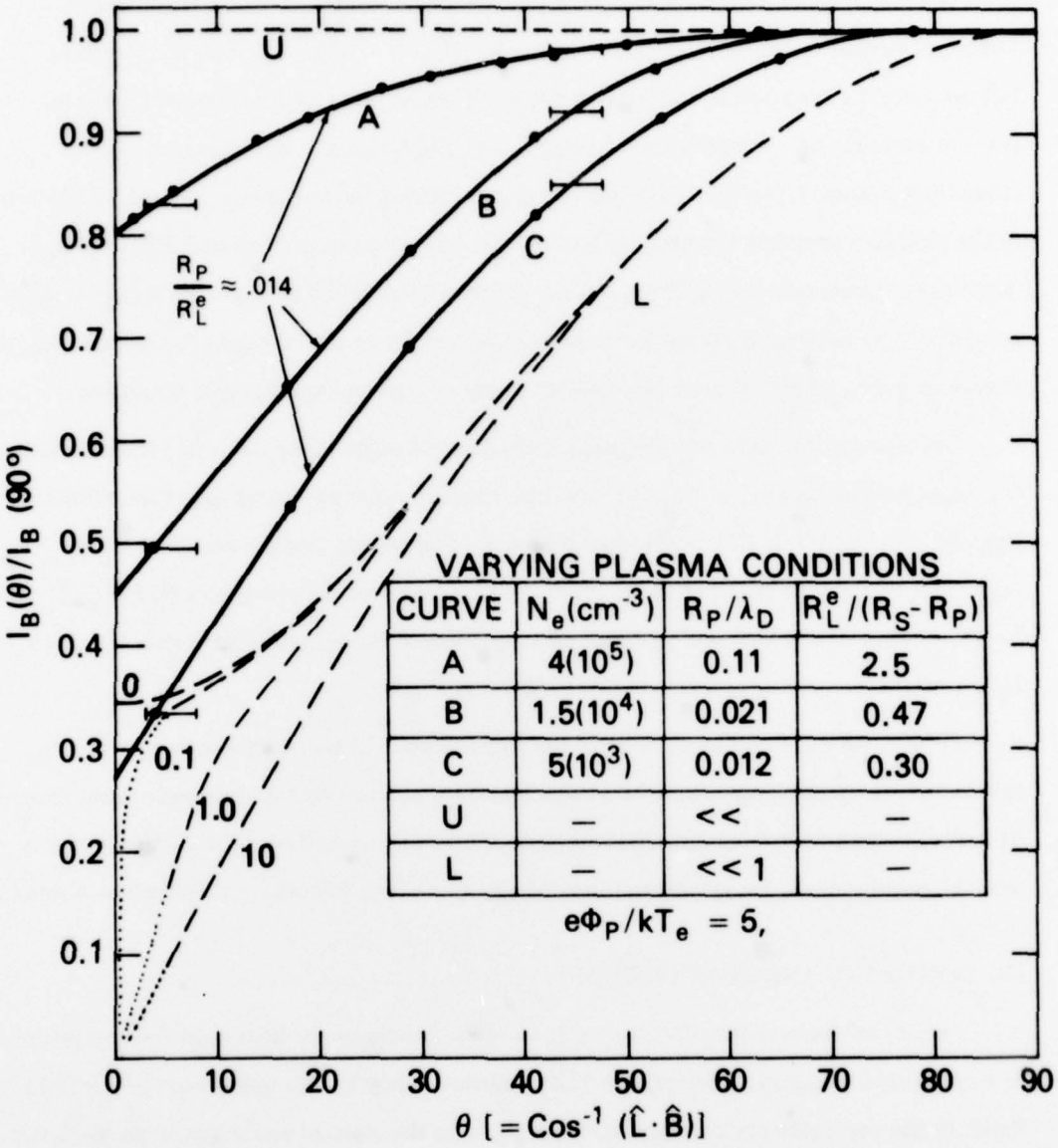

Fig. 4 — Experimental (curves A, B, and C) and theoretical (curves U and L with parametric dependence on R_p/R_L^e) results showing the effect of magnetic aspect on cylindrical electron-collecting probe current. The L-curves at $\theta \geq 5^\circ$ are taken from Ref. 12 with dotted extrapolations to $\theta = 0^\circ$ based on Eq. (6) in the same reference.

The experimental results in Fig. 4 (Curves A, B, and C) were all collected under conditions for which $R_p/R_L^e \approx 0.014$ and are therefore appropriate for comparison with the Laframboise and Rubinstein curves U, and $L(R_p/R_L^e, \theta) = L(0, \theta)$, $L(0.1, \theta)$. The data fall between the theoretical limits (with the qualification on small θ discussed here) and provide evidence of a continuous variation from conditions of a weak-magnetosheath (the upper bound, U) to those of a strong-magnetosheath (the adiabatic limit, L). The trend in the data also supports the premise advanced in the previous section that $R_L^e/(R_s - R_p)$ is an approximate measure of $R_L^e/(\varphi/|\nabla\varphi|)$ where $\varphi/|\nabla\varphi|$ is the gradient scale size of sheath potential. The analytic formulation in Eq. (7) is therefore a useful gauge for determining the degree to which adiabatic limit calculations apply to a given experimental condition.

The trend in the data and the minimum observed value of $R_L^e/(R_s - R_p)$ indicate that the experimental conditions did not meet the guidelines for having achieved the adiabatic limit $R_L^e/(R_s - R_p) \ll 1$. We would infer that with increasingly smaller values of $R_L^e/(R_s - R_p)$ experimental curves operating under thick sheath conditions would approach $L(R_p/R_L^e, \theta) = L(0.1, \theta)$ for $\theta \gtrsim 5°$. At $\theta = 0°$, a finite nonzero current would result such that $0 < I_B(0°)/I_B(90°) \leqslant 0.28$.

Finally, we note that at no time in our experiment did we observe a "negative resistance" current-voltage characteristic, a feature predicted by the detailed orbital scheme of Laframboise and Rubinstein. This supports their position and our observation, namely that the requirements for achieving the adiabatic limit [our inequality (7b)] are very severe.

IV. COMMENTS AND CONCLUSIONS

Arguments have shown that the extent to which a magnetic field modifies the response of a cylindrical Langmuir probe cannot be measured solely by the magnitude of the field itself. In the past, primary concern has been given to the ratio of probe radius to the Larmor radius in efforts to define weak-, strong-, and transition-field response. We have shown that an equally important consideration is the ratio of Larmor radius to sheath thickness, and have established appropriate inequalities (7a), (7b), and (7c) involving not only the magnetic field strength, but also the plasma parameters of density and temperature, and the

applied probe potential. Our results suggest that the regions of operation are more appropriately defined as weak-, strong-, and transition-magnetosheath in order to more clearly stipulate the interacting phenomena. We have shown that a 0.25 G field can have the same perturbing influence on a cylindrical probe applied to ionospheric plasma densities as a 30 kG field would have in a hot, dense laboratory plasma.

Our experimental results are in agreement with the criteria [Eq. (7a-c)] which define the various regions of response. In particular, the results reveal potential problems in the use of fixed-bias probes as indicators of changes in relative electron densities in a magnetoplasma. Because sheaths expand and contract as plasma densities fall and rise, the ratio of gyroradius-to-sheath thickness varies and modifies the probe response in a nonlinear way. One must therefore guarantee weak-magnetoplasma conditions (7a) before assuming $I_e = KN_e$.

Our results have also demonstrated the importance of sheath thickness on the response of cylindrical probes as a function of probe orientation relative to the ambient magnetic field. We have shown that the percent modulation, i.e., $M \equiv 100 \times \left[I_e(90°) - I_e(0°)\right] / I_e(90°)$, increases with sheath thickness. This result is in agreement with the upper bound and adiabatic limit calculations of Laframboise and Rubinstein and provides useful guidelines for determining the degree to which the opposing limits are met. In particular, a comparison between theory and experiment shows that our weak- and strong-magnetosheath conditions are in effect identical to their upper bound and adiabatic limits respectively. Using the criteria expressed by the inequalities in (7), our experimental conditions did not satisfy the guidelines for having achieved the adiabatic limit, a result consistent with the non-existence of a "negative resistance" characteristic ($dI_e^{sat}/d\varphi_p < O$) in our data. This supports the Laframboise and Rubinstein position that the requirements for achieving the adiabatic limit [our inequality (7b)] are very severe.

Finally, our results indicate that $I_e(\theta \approx 90°)$ is a better measurement of electron density variations than $I_e(\theta \ll 60°)$. However, without an independent measurement of N_e, it is impossible to establish the absolute accuracy. We suggest that this area be

approached with caution, particularly any use of standard analysis techniques in the electron saturation region for making absolute measurements of ambient electron density.

ACKNOWLEDGMENTS

The ionospheric data reported in this work was collected as part of Project Antarqui, a major equatorial study coordinated by NASA with Dr. Richard Goldberg as Project Scientist. We wish to thank Dr. Goldberg and his team of engineers and technicians for their support throughout the program. We also wish to thank Mr. J. C. Holmes, and Drs. Golden and Walker for their helpful suggestions in the review and development of this work which was supported in part by NASA Code ST under contract W-14,252.

REFERENCES

1. R.L.F. Boyd, in *Plasma Diagnostics*, edited by W. Lochte-Holtgreven (North-Holland, Amsterdam, 1968), p. 732.
2. F.F. Chen, in *Plasma Diagnostic Techniques*, edited by R.H. Huddlestone and S.L. Leonard, (Academic New York, 1965), p. 113.
3. L. Schott, in *Plasma Diagnostic Techniques*, edited by R.H. Huddlestone and S.L. Leonard, (Academic New York, 1965), p. 668.
4. C.V. Goodall and D. Smith, Plasma Phys. **10**, 249 (1968).
5. E.P. Szuszczewicz, J. Appl. Phys. **43**, 874 (1972).
6. J.C. Holmes and E.P. Szuszczewicz, Rev. Sci. Instrum. **46**, 592 (1975).
7. F. Waymouth, J. Appl. Phys. **37**, 4492 (1966).
8. J.R. Sanmartin, Phys. Fluids **13**, 103 (1970).
9. I.G. Brown, A.B. Compher, and W.B. Kunkel, Phys. Fluids **14**, 1377 (1971).
10. F.F. Chen, C. Etievant, and D. Mosher, Phys. Fluids **11**, 811 (1968).
11. N.J. Miller, J. Geophys. Res. **77**, 2851 (1972).

12. J.G. Laframboise and J. Rubinstein, Phys. Fluids **19**, 1900 (1976); information for the figures was taken from a more detailed report published under the same title as Rpt. No. 061060-12-T, Space Physics Research Laboratory, Dept. of Atmospheric and Oceanic Science, University of Michigan (June 1976).
13. J.G. Laframboise, University of Toronto Institute of Aerospace Studies, Report No. 100 (1966).
14. J.H. de Leeuw, in *Physico-Chemical Diagnostics of Plasmas*, edited by T.P. Anderson, R.W. Springer, and R.C. Warder, Jr. (Northwestern University Press, Evanston, Ill., 1963), p. 65.
15. A.A. Sonin, AIAA J. 4, 1588 (1966).
16. R.T. Bettinger and E.H. Walker, Phys. Fluids 8, 748 (1965).
17. E.P. Szuszczewicz and J.C. Holmes, J. Appl. Phys. **46**, 5134 (1975).
18. E.P. Szuszczewicz and J.C. Holmes, AIAA Paper No. 76-393, (1976).
19. E.P. Szuszczewicz and J.C. Holmes, J. Geophys. Res. 82, 5073 (1977).
20. E.P. Szuszczewicz, D.N. Walker, J.C. Holmes, and H. Leinbach, Geophys. Res. Lett. **6**, 201 (1979).
21. D.N. Walker, E.P. Szuszczewicz, and J.C. Holmes, NRL Memorandum Report No. 3649 (1977).